Dalton Transactions

PAPER

View Article Online
View Journal | View Issue

Cite this: *Dalton Trans.*, 2017, **46**, 16190

Optical limiters with improved performance based on nanoconjugates of thiol substituted phthalocyanine with CdSe quantum dots and Ag nanoparticles†

David O. Oluwole,[a] Alexey V. Yagodin,[b,c] Jonathan Britton,[a] Alexander G. Martynov,[c] Yulia G. Gorbunova,*[c,d] Aslan Yu. Tsivadze[c,d] and Tebello Nyokong*[a]

Received 13th October 2017,
Accepted 31st October 2017

DOI: 10.1039/c7dt03867d

rsc.li/dalton

Two alternative synthetic approaches affording a low-symmetry A_3B-type phthalocyanine **1** bearing two [2′-(2″-mercaptoethoxy)ethoxy] anchoring substituents were developed. Due to the presence of thiol groups, this phthalocyanine could be conjugated with TOPO-capped (TOPO - trioctylphosphine)-capped CdSe quantum dots (**CdSe-QDs**) or oleylamine capped silver nanoparticles (**Ag-NPs**). The nonlinear optical behaviour of starting phthalocyanine, quantum dots, nanoparticles and their conjugates was studied by using an open aperture *Z*-scan technique, revealing that the grafting of **1** onto the nanomaterials resulted in a significant enhancement of the optical limiting of **1-Ag** and **1-CdSe** in comparison with the individual components. The conjugate **1-CdSe**, being the first example of Pc-based thiol conjugated with quantum dots, revealed superior limiting characteristics with a limiting threshold below 0.18 J cm^{-2}.

Introduction

Optical limiting (OL) materials are important in protecting light sensitive materials from intense laser beams.[1–6] The materials for OL are required to have some desirable nonlinear optical (NLO) properties which include large nonlinear absorption coefficients and fast response times to provide efficient optical limiting.

Among the organic molecules that have been exploited for OL application, phthalocyanines (Pcs) have proven to be excellent NLO materials.[1,7–10] This is due to their excellent photophysical properties and optical nonlinearities provided by the extended π-electron conjugated system, as well as high thermal and chemical stability, wide possibilities of synthesis and structural modification.[11] The tuning of the NLO properties of Pcs can be achieved by varying the nature of the central metal in the cavity of the Pc ring, by altering the ring substituents or by lowering the molecular symmetry.[12–15] For example, phthalocyanines containing heavy central metals such as In, Ga or Zn show improved NLO behaviour due to increased intersystem crossing as a result of the heavy atom effect.[8,16,17] On the other hand, metal free phthalocyanines are also known to possess good NLO behaviour as a result of the lack of symmetry.[18]

Nanoparticles (NPs) and quantum dots (QDs) are also promising optical materials due to their quantum confinement.[19–24] Conjugation of Pcs with nanomaterials improves the NLO behaviour of the conjugates in comparison with the parent species.[25–27] Such conjugation typically requires the introduction of certain anchoring groups into the Pcs, and several examples of Pcs conjugated with QDs *via* amide or ester bonds have been previously reported, however, to the best of our knowledge the conjugates of QDs with thiolated Pcs have not been described. At the same time, thiolation of various organic substrates is a powerful tool for their further conjugation with nanoparticles, metal surfaces, *etc.*[28,29] Thiolated Pcs have been shown to be valuable components of such conjugates, acting as sensors,[30] photosensitizers,[31] hole injectors,[32] *etc.*

In the present study we report the synthesis of the novel low-symmetry phthalocyanine **1**, starting from the recently published A_3B-type ligand **2**,[18] bearing two diethyleneglycol chains with terminal OH-groups (Scheme 1). The asymmetry of ligand **2** and its complexes was shown to improve its NLO

[a]*Department of Chemistry, Rhodes University, Grahamstown 6140, South Africa. E-mail: t.nyokong@ru.ac.za*
[b]*Dmitry Mendeleev University of Chemical Technology of Russia, Miusskaya sq., 9, 125047 Moscow, Russia*
[c]*A. N. Frumkin Institute of Physical Chemistry and Electrochemistry, Russian Academy of Sciences, Leninskii pr., 31, bldg. 4, Moscow, 119071, Russia. E-mail: Martynov.Alexandre@gmail.com*
[d]*Kurnakov Institute of General and Inorganic Chemistry, Russian Academy of Sciences, Leninskii pr., 31, Moscow, 119991, Russia. E-mail: yulia@igic.ras.ru*

†Electronic supplementary information (ESI) available: ^{1}H-NMR, UV-Vis, FT-IR, MALDI TOF MS, EDX data for synthesized compounds and conjugates. See DOI: 10.1039/c7dt03867d

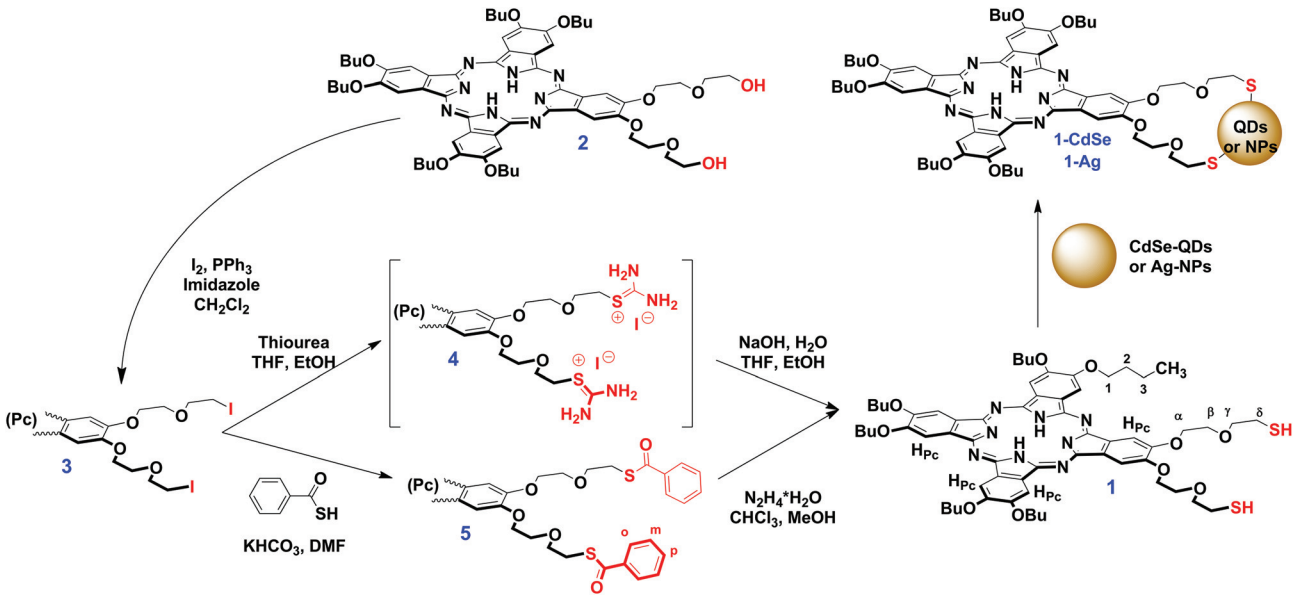

Scheme 1 Approaches to the synthesis of phthalocyanine **1** bearing two [2′-(2″-mercaptoethoxy)ethoxy] substituents and the conjugation of **1** with quantum dots and nanoparticles together with the numbering of protons, used in the assignment of the ^{1}H-NMR spectra.

behaviour in comparison with symmetrical phthalocyanines,[18,33] therefore we aimed to study the OL properties of the thiolated derivative **1** and to investigate the influence of its conjugation with various nanomaterials. This was studied herein on the examples the nanoconjugates **1-CdSe** and **1-Ag** which were formed by the interaction of **1** with trioctylphosphine oxide (TOPO) capped CdSe quantum dots (**CdSe-QDs**) and oleylamine capped silver nanoparticles (**Ag-NPs**). The nonlinear optical behaviour of the starting materials and conjugates was studied by using the open aperture *Z*-scan technique.

Results and discussion

Synthesis and characterization of phthalocyanines

Two major approaches of Pc thiolation were previously reported, namely the reaction of Pcs bearing terminal leaving groups with thiourea and the subsequent hydrolysis of the intermediate thiouronium salt[32,34,35] or the direct functionalization of Pcs with thiol-containing fragments.[31]

Using the first approach, we started the synthesis of the target thiolated phthalocyanine **1** from the previously reported A_3B-type ligand **2**, which was shown to exhibit prominent NLO properties due to the low molecular symmetry. To introduce the leaving groups, we treated the parent Pc **2** with iodine, triphenylphosphine and imidazole in DCM (Scheme 1). It afforded a diiodide derivative **3**, which was isolated in 84% yield after column chromatography. The reaction of **3** with thiourea in the THF/EtOH mixture afforded the corresponding thiouronium salt **4** which was hydrolyzed without isolation with aqueous NaOH solution. The isolation of the dithiol **1** by column chromatography afforded the target compound in a moderate yield (39%). However, the harsh conditions of this reaction might preclude the application of this approach in the case of more sophisticated Pcs, like sandwich complexes, which are less tolerant to hydrolysis in strongly polar media.[36–38]

With the aim to improve the abovementioned drawbacks, we have proposed another approach, which implied the substitution of iodine atoms with thiobenzoyl fragments and the subsequent mild cleavage of benzoyl protective groups (Scheme 1).[39] The treatment of **3** with thiobenzoic acid in the presence of excess of $KHCO_3$ in DMF afforded thiobenzoylated Pc **5** which was isolated in 89% yield. The previously reported procedure of the deprotection of benzoyl groups with hydrazine hydrochloride and sodium acetate in DMF[39] failed to furnish the target dithiol **1**, however, Pc **5** could be smoothly and quantitatively deprotected by using hydrazine hydrate in the $CHCl_3$/MeOH mixture.

Compounds **1**, **3** and **5** were characterized by MALDI TOF MS, ^{1}H-NMR, UV-Vis and FT-IR spectra and elemental analysis, which were in full agreement with the proposed structures (Fig. S1–S9†). ^{1}H-NMR spectroscopy evidenced the non-equivalence of aromatic protons of the phthalocyanine macrocycle in low-symmetry ligands **1**, **3** and **5** (Fig. 1, S1 and S5†), which arises from slightly different electronic effects of the butoxy group and the diethyleneglycol chain.[18,33] In turn, it results in dissymmetry in the distribution of the electronic density over the ligand, which provides starting Pc **2** and its complexes with the enhanced NLO properties.[18,33]

Although the presence of the SH-group in **1** was confirmed by FT-IR (a weak band at 2556 cm^{-1}) and NMR spectra (triplet signal at 1.92 ppm and J = 8.2 Hz), in the MALDI-TOF mass-spectrum we observed the set of molecular ions $[(M - 2H)_n]^+$ with n = 1–3, which could correspond to the oxidative dimerization of SH-groups under the MS experimental conditions (Fig. S9†).

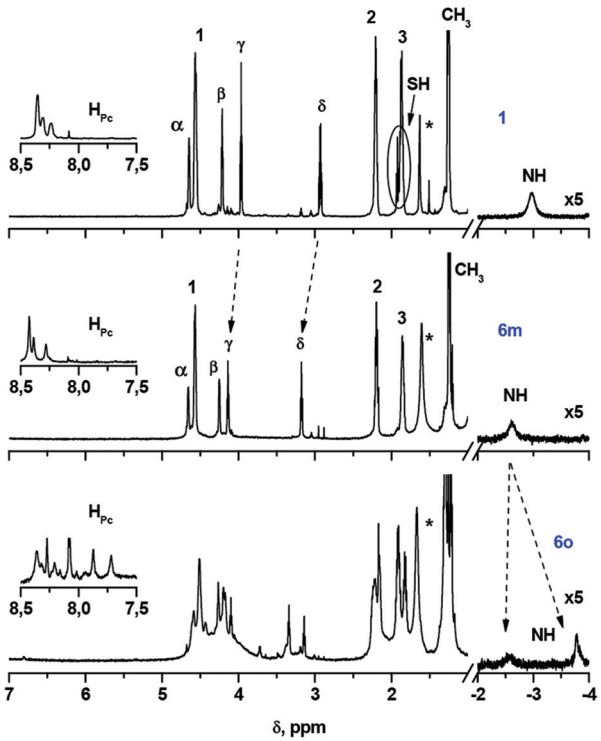

Fig. 1 ^{1}H-NMR spectra of phthalocyanines **1**, **6m** and **6o** in $CDCl_3$. The numbering of protons is given in Scheme 1. The insets show the resonance signals of aromatic protons. Asterisk marks show the residual water signal.

Moreover, the oxidation of **1** with the formation of disulphide derivatives with S–S bonds proceeded slowly upon the aerobic storage of **1** (Scheme 2). This feature is well-known in thiol chemistry and in our case the formation of disulphides can be facilitated due to the generation of singlet oxygen promoted by the phthalocyanine. Dithiol **1** can undergo the intra-/intermolecular oxidative coupling of SH-groups with the formation of dithiacrown-ether macrocycles.[40] In contrast, the benzoylated ligand **5** is air stable, which makes the proposed pathway to the synthesis of thiolated Pcs more convenient in comparison with the methodology involving thiourea.[41]

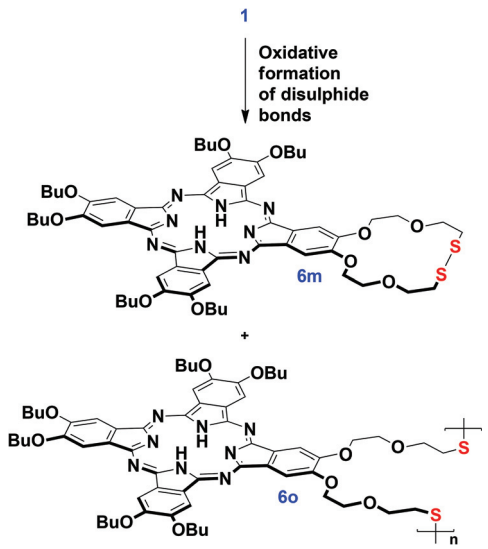

Scheme 2 Formation of phthalocyanines **6m** and **6o** upon the oxidative formation of disulphide bonds.

We managed to separate the mixture of oxidation products and isolate the essentially pure monomeric phthalocyanine **6m** and the mixture of oligomeric species **6o** by size-exclusion chromatography on BioBeads S-X1. According to MALDI TOF MS, the fraction **6o** contained the species from a dimer to a tetramer. ^{1}H-NMR characterization of the isolated fractions indeed evidenced the disappearance of SH-group resonance in both fractions as well as the appearance of the complicated set of resonance signals in the spectrum of **6m** and the splitting of the NH proton signal (Fig. 1). The broad Q-band, which was observed in the UV-Vis spectrum of **6o**, is in agreement with the proposed oligomeric structure,[42] while the UV-Vis spectrum of **6m** was typical of monomeric phthalocyanines (Fig. S10†).

Nevertheless, the formation of disulphides is not an obstacle for further binding to nanomaterials, since they undergo easy reductive cleavage with the formation of metal–sulphur bonds.[28–30]

Conjugation of phthalocyanine 1 with quantum dots and nanoparticles

The reaction of **1** with **CdSe-QDs** and **Ag-NPs** proceeded in DCM solution *via* the substitution of TOPO and oleylamine ligands with thiols. This process was followed by the disappearance of the SH vibration band and the bands of capping ligands in the FT-IR spectra of **1-CdSe** and **1-Ag** conjugates, which suggested the formation of metal–sulphur bonds (Fig. 2).

The UV-Vis spectrum of **1** alone consisted of well-resolved split Q-bands at 699 nm and 662 nm, which is typical of a monomeric metal-free Pc, but in the UV-Vis spectra of **1-CdSe** and **1-Ag**, the Pc Q-band regions were dominated by a broad band below 640 nm (Fig. 3). This band might be assigned both to the interaction between the electronic systems of Pc, QDs or NPs, as well as the aggregation of Pc molecules, absorbed on the surface of nanomaterials. The observed enhancement in the UV–Vis absorption spectra of the conjugates (**1-CdSe** and **1-Ag**) around 350 nm to 650 nm compared to compound **1** alone could also be attributed to the presence of **CdSe-QDs** and **Ag-NPs** in the respective conjugates which absorb around 350 nm to 650 nm. This is evidenced by using the overlay of UV–Vis absorption for **CdSe-QDs**, **1** and their conjugates and further corroborated by XRD and TEM (Fig. 4 and 5). The presence of all expected elements was confirmed by EDX spectra (Fig. S11†).

The XRD pattern of the conjugates resembled the patterns of both **1** and QDs or NPs (Fig. 4 showing the example of **1-CdSe**). The XRD diffractogram of **CdSe-QDs** alone confirmed the presence of three prominent diffraction patterns with 2θ values (2θ = 25.29°, 42.29° and 49.86°) corresponding to the

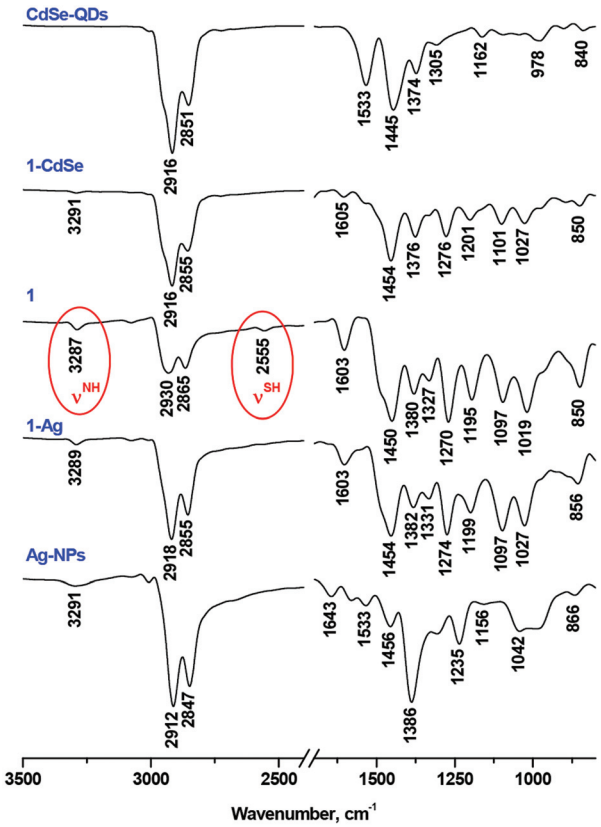

Fig. 2 FT-IR spectra of starting phthalocyanine **1**, TOPO-capped **CdSe-QDs**, oleylamine-capped **Ag-NPs** alone and conjugates **1-CdSe** and **1-Ag**. NH stretching in the FT-IR spectrum of **Ag-NPs** arises from the oleylamine capping ligand.

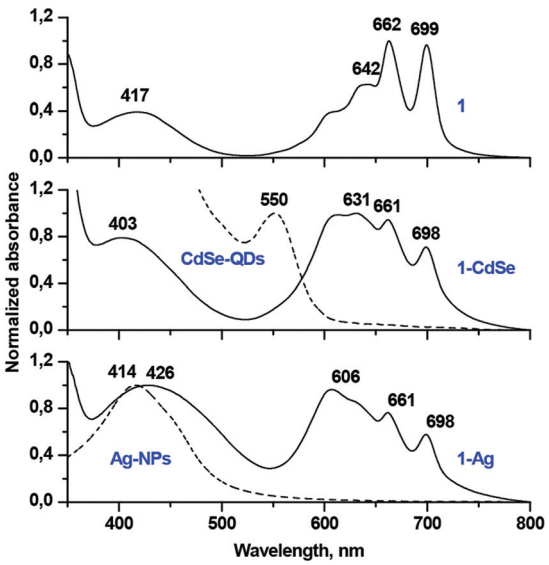

Fig. 3 Normalized UV-Vis spectra of phthalocyanine **1**, TOPO capped CdSe quantum dots, oleylamine capped silver nanoparticles alone, conjugates **1-CdSe** and **1-Ag** in DCM.

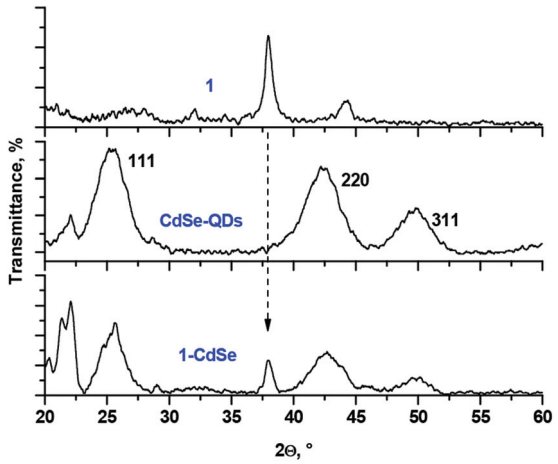

Fig. 4 XRD spectra of phthalocyanine **1**, TOPO-CdSe quantum dots and conjugate **1-CdSe**.

zinc blend crystal and cubic structure at planes 111, 220 and 311, respectively. The size of the **CdSe-QDs** (3.8 nm) was calculated based on the Debye–Scherrer equation.[43] The nanoconjugate **1-CdSe** also showed a similar diffraction pattern to the **CdSe-QDs**, but with additional sharp peaks which could imply an increase in crystallinity upon linking to Pcs. Ligand **1** alone showed crystalline peaks and this is expected for Pcs as reported in the literature.[44]

TEM measurements were used to characterize both starting QDs and NPs as well as the resulting conjugates (Fig. 5). The size of particles, found by TEM is close to those found by XRD. In the case of **1-Ag** the aggregation of nanoparticles upon conjugation was observed which could alter the optical properties of the conjugates.[45,46]

Measurements of nonlinear optical properties

Fig. 6 shows the examples of the open aperture *Z*-scan profile spectra of **Ag-NPs** and Pc **1** alone as well as the **1-Ag** conjugate, recorded at 532 nm with a 10 ns laser pulse in DCM. From the spectra, we can conclude that compound **1** and its nanoconjugate exhibit reverse saturable absorption (RSA) which is typical of phthalocyanines.[4,12] The normalized transmittance of **1-Ag** exhibited a deeper valley compared to complex **1** alone and Ag-NPs alone, suggesting a better OL performance of the conjugate. Similar results were obtained for **CdSe-QDs** and the **1-CdSe** conjugate.

The imaginary third-order nonlinear susceptibility $\mathrm{Im}[\chi^{(3)}]$ was calculated from the two photon absorption coefficient β_{eff}; the values are listed in Table 1. $\mathrm{Im}[\chi^{(3)}]$ is related to the hyperpolarizability γ which measures the interaction of the incident photon with the permanent dipole moments of the Pcs. $\mathrm{Im}[\chi^{(3)}]$ measures the response time of a NLO material, following the perturbation initiated by the intense laser pulses. An efficient optical limiting material must have high γ and/or $\mathrm{Im}[\chi^{(3)}]$ as well as β_{eff}. It was shown that the β_{eff} and $\mathrm{Im}[\chi^{(3)}]$ are improved for **1** in the presence of QDs or NPs. The β_{eff} and $\mathrm{Im}[\chi^{(3)}]$ values of the conjugates (**1-CdSe** and **1-Ag**) were

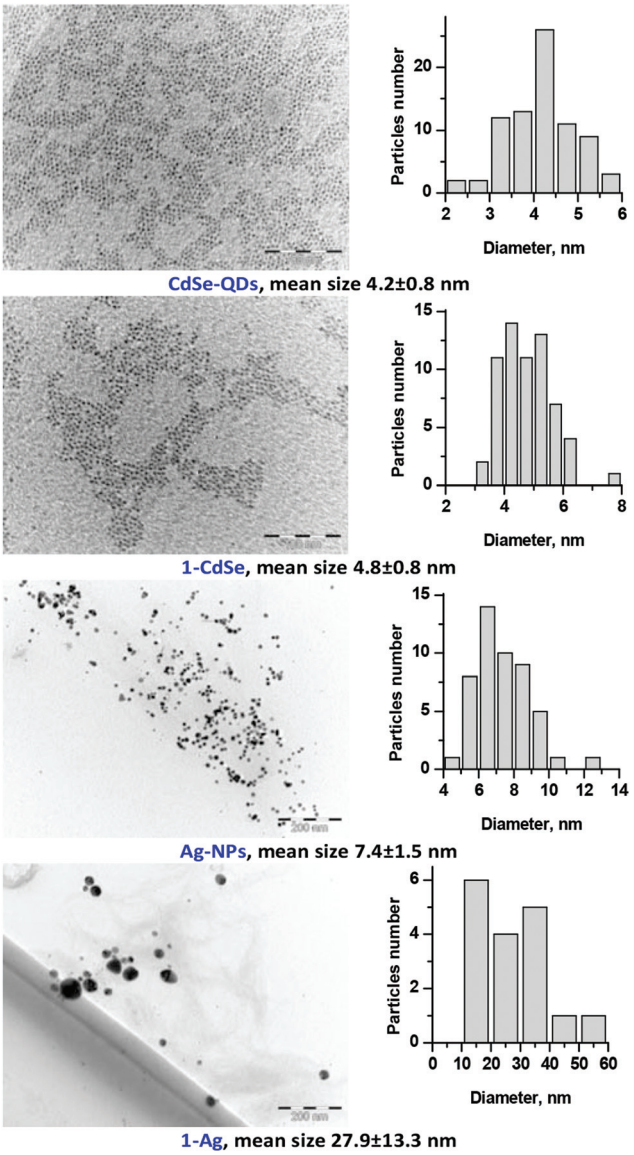

Fig. 5 TEM images and the corresponding size distributions of TOPO-CdSe quantum dots, oleylamine-capped Ag nanoparticles and conjugates **1-CdSe** and **1-Ag**.

Table 1 Nonlinear optical data of phthalocyanine **1**, **CdSe-QDs**, **Ag-NPs** and conjugates **1-Ag** and **1-CdSe** in DCM. I_o = ~0.25 GW cm^{-2} (55 μJ)

Compound	β_{eff} (m W^{-1})	Im[$\chi^{(3)}$] (esu)	I_{lim} (J cm^{-2})
1	3.61×10^{-8}	3.09×10^{-11}	1.35
1-CdSe	7.30×10^{-8}	6.26×10^{-11}	0.18
1-Ag	5.76×10^{-8}	4.94×10^{-11}	0.43
CdSe-QDs	3.00×10^{-9}	2.57×10^{-12}	[a]
Ag-NPs	1.53×10^{-8}	1.31×10^{-11}	[a]

[a] 50% attenuation of the transmitted fluence is not achieved.

superior to those of the NPs or compound **1** alone, as shown in Table 1. This trend further lay credence to the synergistic activity that can be achieved when nanomaterials are linked to phthalocyanines.

The investigated OL material displayed a decreasing transmittance as a function of the incident fluence (Fig. 7). At a low incident fluence, the material has a linear transmittance; while at some critical fluence or threshold, the transmittance changes abruptly, and leads to the clamping of the output fluence at a constant value that would presumably be less than the amount required to damage the optical element.[5] This critical point is referred to as the threshold limit intensity or fluence (I_{lim}).[5] The lower the I_{lim} values the better is the material as an optical limiter. The I_{lim} value decreased (Table 1) for the conjugates as compared to complex **1** alone, particularly indicating a superior optical limiting behaviour for the **1-CdSe** composite material. 50% attenuation of the transmitted fluence is not achieved for the nanomaterials which show their deficiency when used alone since their conjugates with Pcs exhibited an improved limiting threshold pivotal for optical nonlinearity.

The improvement of OL in conjugates can be attributed to several factors. In the case of QDs, they absorb at 532 nm where the NLO behaviour was studied, therefore QDs can contribute to the NLO behaviour of Pcs due to the free-carrier absorption (FCA) mechanism, which is usually produced when excitation takes place at the wavelengths where there is linear

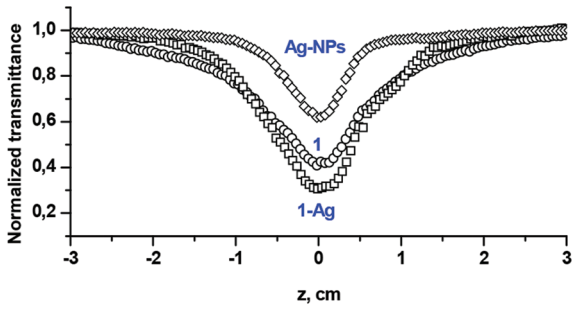

Fig. 6 Open aperture *Z*-scan curves for **Ag-NPs**, phthalocyanine **1** and conjugate **1-Ag**. All measurements were carried out in dichloromethane (absorbance 2.0) at 532 nm with a pulse rate of 10 ns with I_o = ~0.25 GW cm^{-2}.

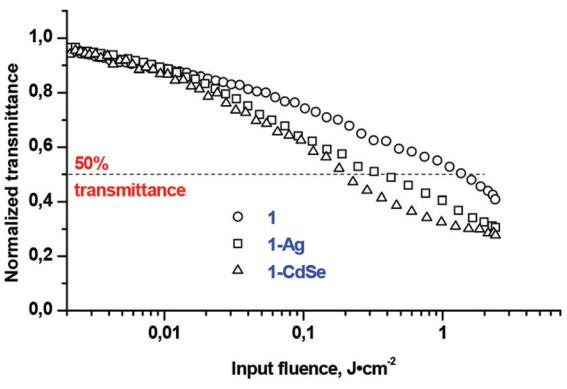

Fig. 7 Normalized transmittance *versus* input fluence curves for phthalocyanine **1** and conjugates **1-Ag** and **1-CdSe**. All measurements were carried out in dichloromethane (absorbance 2.0) at 532 nm with a pulse rate of 10 ns with I_o = ~0.25 GW cm^{-2}.

absorption.[26] Second, QDs and NPs may improve the NLO behaviour of Pcs due to the heavy atom effect which improves the triplet state population which directly affects the NLO behaviour. Finally, the aggregation of Pc chromophores in the vicinity of nanomaterials deduced from the UV-Vis spectra may also contribute to the enhancement of OL.[45] Further studies might give more information about the synergistic effects which arise from electronic interaction between the phthalocyanine chromophore and quantum dots or nanoparticles.

Conclusions

We report for the first time, two synthetic approaches towards bis-[2′-(2″-mercaptoethoxy)ethoxy]-substituted phthalocyanine **1**, based on the thiolation of diiodo-derivative **3** – either by a conventional and relatively harsh reaction with thiourea and the subsequent hydrolysis of the intermediate thiouronium salt, or by a mild reaction of **3** with thiobenzoic acid and the quantitative deprotection of **5** with hydrazine. We envisage that the latter method can be used for the synthesis of more sophisticated thiolated Pcs which may not tolerate the conditions of the former approach.

Dithiol **1** was conjugated with CdSe quantum dots and silver nanoparticles to study their effects on the nonlinear optical characteristics of the phthalocyanine chromophore within the nanoconjugates by the *Z*-scan technique. The two photon absorption mechanism of optical limiting was confirmed and the characteristic values of $\mathrm{Im}[\chi^{(3)}]$ and β_{eff} were found. It is evidenced that the combination of **1** with QDs and NPs showed improved NLO behaviour compared to individual components. The mechanisms of this enhancement were discussed.

Experimental

Materials and methods

2,3-Bis[2′-(2″-hydroxyethoxy)ethoxy]-9,10,16,17,23,24-hexa-*n*-butoxyphthalocyanine **2** was synthesized starting with 4,5-bis[2′-(2″-hydroxyethoxy)ethoxy]benzene[47] and 4,5-di-*n*-butoxyphthalonitrile according to the previously reported procedure.[18] TOPO-capped **CdSe-QDs** and oleylamine-capped **Ag-NPs** were synthesized as reported in the literature.[48,49]

Dichloromethane (DCM) was distilled over CaH_2 under argon. Chloroform was stored over $NaHCO_3$ and distilled over K_2CO_3 to remove acidic impurities. Tetrahydrofuran (THF) was distilled over Na/benzophenone under argon. Ultrapure water was obtained from a Milli-Q Water System (Millipore Corp., Bedford, MA, USA). Other chemicals (Merck, Aldrich), silica (Macherey Nagel) and BioBeads S-X1 (BioRad) were used as received from commercial suppliers.

The mass spectral data were acquired on a Bruker® Daltonics Ultraflex spectrometer with 2,4-dihydroxybenzoic acid as the matrix. A mass spectrometer operated in a positive ion mode using an *m*/*z* range of 500–5000 amu. NMR spectra were recorded with a Bruker Avance 600 spectrometer. NMR spectra were referenced against the residual solvent signal.[50]

Ground state electronic absorption was measured on Shimadzu UV-2550 and Thermo Evolution 201 spectrophotometers. FT-IR spectra were recorded on Bruker ALPHA FT-IR and Nexus Nicolet spectrometers with universal attenuated total reflectance (ATR) sampling accessories. X-ray powder diffraction patterns were recorded using Cu Kα radiation (1.5405°A, nickel filter) equipped with a Lynx Eye detector, on a Bruker® D8 Discover equipped with a proportional counter and the X-ray diffraction data were processed using the Eva (evaluation curve fitting) software. Elemental analyses were carried out on a EuroVector EA-3000 CHNS analyzer. The morphology of nanoparticles was assessed using a transmission electron microscope, ZEISS LIBRA® model 120, operated at 90 kV accelerating voltage. *Z*-Scan experiments were carried out as described in the literature using a frequency-doubled Nd:YAG laser (Quanta-Ray, 1.5 J/10 ns fwhm pulse duration) as the excitation source. Details have been provided previously.[51]

Elemental analysis, MALDI TOF MS, NMR and FT-IR measurements were performed at the Shared Facility Centres of the A.N. Frumkin Institute of Physical Chemistry and Electrochemistry, RAS, and the N.S. Kurnakov Institute of General and Inorganic Chemistry, RAS.

2,3-Bis[2′-(2″-iodoethoxy)ethoxy]-9,10,16,17,23,24-hexa-*n*-butoxyphthalocyanine 3

Iodine (105 mg, 0.42 mmol) was weighed in a round bottom flask, 5 mL of DCM was added and the reaction mixture was stirred at an ambient temperature for 10 min, followed by the addition of triphenyphosphine (113 mg, 0.43 mmol). The reaction mixture was stirred for 30 min and then imidazole (56.5 mg, 0.75 mmol) was added into the reaction mixture which was allowed to stir for 10 min. The flask with the formed yellow suspension was protected from light with foil. Phthalocyanine **2** (100 mg, 87 μmol) was added and the mixture was stirred overnight. The progress of the reaction was monitored by thin layer chromatography (TLC). Upon completion, aqueous Na_2SO_3 solution was added and the mixture was stirred for 10 min to quench the excess of the iodinating reagent. The organic layer was separated, washed with water and evaporated to give a dark-green residue. The iodinated derivative **3** was isolated by column chromatography on silica (elution with the mixture of $CHCl_3$ + 1 vol% MeOH) as a dark-green solid (yield – 102 mg, 84%). MALDI TOF MS: calculated for $C_{64}H_{80}I_2N_8O_{10}$ – 1374.5, found – 1374.4 $[M]^+$. ^{1}H NMR (600 MHz, $CDCl_3$) δ 8.35, 8.34, 8.26 and 8.15 (4s, 2 × 2H, H_{Pc}), 4.61 (br m, 4H, α-CH_2^{DEG}), 4.58–4.53 (m, 12H, OCH_2^{Bu}), 4.24 (t, J = 4.8 Hz, 4H, β-CH_2^{DEG}), 4.13 and 3.51 (2t, J = 7.0 Hz, 2 × 4H, OCH_2CH_2I), 2.23–2.19 (m, 12H, 2-CH_2^{Bu}), 1.97–1.77 (m, 12H, 3-CH_2^{Bu}), 1.28–1.25 (m, 12H, CH_2), −3.05 (br s, 2H, NH). UV-Vis ($CHCl_3$) λ_{max} (lg ε): 702 (5.14), 665 (5.07), 603 (4.41), 426 (4.55), 348 (4.92), 296 (4.76). FT-IR, cm^{-1}: 3290 (w, N–H stretching), 2955 (m), 2930 (m), 2869 (m), 1603 (m), 1536 (w), 1482 (s), 1444 (s), 1381 (s), 1328 (s), 1273 (s), 1197 (s), 1096 (s), 1020

(s), 932 (m), 852 (s), 796 (m), 739 (s), 691 (s), 613 (w), 576 (w). Elemental analysis (%): calc. for $C_{64}H_{80}I_2N_8O_{10}$ (**3**): C, 55.90; H, 5.86; N, 8.15. Found: C, 55.47; H, 5.91; N, 8.33.

2,3-Bis[2′-(2″-benzoylthioethoxy)ethoxy]-9,10,16,17,23,24-hexa-*n*-butoxyphthalocyanine 5

Diiodide **3** (21 mg, 15 μmol) was suspended in 3 ml DMF, thiobenzoic acid (17 mg, 0.123 mmol) and $KHCO_3$ (18 mg, 0.18 mmol) were added. The mixture was flushed with argon and heated to 45 °C overnight. Upon the completion of the reaction, which is confirmed by MALDI-TOF mass-spectrometry, the reaction mixture was diluted with water; the obtained green precipitate was filtered and washed off the filter with chloroform. The thiobenzoylated derivative **5** was isolated by column chromatography on silica (elution with the mixture of $CHCl_3$ + 1 vol% MeOH) and size-exclusion chromatography in BioBeads S-X1 (elution with the mixture of $CHCl_3$ + 2.5 vol% MeOH) as a dark-green solid (yield – 19 mg, 89%). MALDI TOF MS: calculated for $C_{78}H_{90}N_8O_{12}S_2$ – 1394.6, found – 1394.8 $[M]^+$. ^{1}H NMR (600 MHz, $CDCl_3$) δ, ppm: 8.25–8.20 (m, 8H, H_{Pc}), 8.00 (d, J = 7.7 Hz, 4H, *o*-CH), 7.46 (t, J = 7.3 Hz, 2H, *p*-CH), 7.36 (t, J = 7.7 Hz, 4H, *m*-CH), 4.64 (br s, 4H, α-CH_2^{DEG}), 4.54–4.51 (m, 12H, OCH_2^{Bu}), 4.25 (t, J = 4.7 Hz, 4H, β-CH_2^{DEG}), 4.06 and 3.52 (2t, J = 6.5 Hz, 2 × 4H, OCH_2OCH_2S), 2.22–2.17 (m, 12H, 2-CH_2^{Bu}), 1.89–1.84 (m, 12H, 3-CH_2^{Bu}), 1.27–1.23 (m, 18H, CH_2), −3.29 (s, 2H, NH). UV-Vis ($CHCl_3$) λ_{max} (lg ε): 702 (5.22), 665 (5.14), 603 (4.51), 426 (4.62), 349 (4.99), 295 (4.82). FT-IR, cm^{-1}: 3290 (w, N–H stretching), 2955 (m), 2931 (m), 2870 (m), 1663 (m, C═O stretching), 1601 (m), 1534 (w), 1487 (s), 1445 (s), 1382 (s), 1326 (s), 1275 (s), 1200 (s), 1094 (s), 1026 (s), 909 (s), 851 (s), 796 (m), 740 (s), 689 (s), 648 (m), 616 (w), 575 (w). Elemental analysis (%): calc. for $C_{78}H_{94}N_8O_{14}S_2$ (**5**·2H_2O): C, 65.43; H, 6.62; N, 7.83; S, 4.48. Found: C, 65.74; H, 6.16; N, 8.18; S, 4.44.

2,3-Bis[2′-(2″-mercaptoethoxy)ethoxy]-9,10,16,17,23,24-hexa-*n*-butoxyphthalocyanine 1

Method 1. Diiodide **3** (70 mg, 51 μmol) and thiourea (40 mg, 0.526 mmol) were dissolved in the mixture of 10 ml THF and 3 ml EtOH, the mixture was degassed and refluxed at 80 °C under argon for 5 h to form the thiouronium salt **4**. This salt without isolation was hydrolyzed by the addition of 2 ml of degassed 20% aq. NaOH solution and subsequent refluxing for 2 h. The mixture was neutralized with 0.63 ml of glacial acetic acid. Then it was transferred into the separating funnel, containing 25 ml of H_2O and 10 ml of $CHCl_3$. The organic layer was separated, washed with water and evaporated. The target dithiol **1** was isolated by column chromatography on silica (elution with the mixture of $CHCl_3$ + 0–3 vol% MeOH) as a dark-green solid (yield – 24 mg, 39%).

Method 2. Thiobenzoylated derivative **5** (12 mg, 8 μmol) was dissolved in the mixture of 2.5 ml $CHCl_3$ and 1.25 ml MeOH, 0.1 ml of hydrazine hydrate was added and the mixture was heated to 40 °C under an argon atmosphere overnight. Upon completion of the reaction, confirmed by MALDI-TOF mass-spectrometry, the reaction mixture was washed with water in a separating funnel and the organic layer was evaporated to dryness, yielding target dithiol **1** with quantitatively cleaved protective groups.

MALDI TOF MS: calculated for $C_{64}H_{82}N_8O_{10}S_2$ – 1186.6, found – 1184.5 $[M - 2H]^+$. ^{1}H NMR (600 MHz, $CDCl_3$) δ 8.35, 8.30 and 8.24 (3s, 4H+2×2H, H_{Pc}), 4.65 (br s, 4H, α-CH_2^{DEG}), 4.59–4.54 (m, 12H, OCH_2^{Bu}), 4.21 (t, J = 4.7 Hz, 4H, β-CH_2^{DEG}), 3.97 (t, J = 6.5 Hz, 4H, γ-CH_2^{DEG}), 2.93 (dd, J = 14.4, 6.5 Hz, 4H, δ-CH_2^{DEG}), 2.20 (m, 12H, 2-CH_2^{Bu}), 1.92 (t, J = 8.2 Hz, 2H, SH), 1.89–1.85 (m, 12H, 3-CH_2^{Bu}), 1.28–1.23 (m, 18H, CH_3), −2.98 (s, 2H, NH). UV-Vis (CH_2Cl_2) λ_{max} (lg ε): 700 (4.51), 663 (4.57), 643 (4.46), 419 (4.14), 347 (4.56). FT-IR, cm^{-1}: 3287 (w, N–H stretching), 2930, 2865 (s), 2556 (SH stretching), 1603 (m), 1450 (s), 1380 (m), 1327 (m), 1270 (s), 1195 (m), 1097 (m), 1019 (m), 850 (m). Elemental analysis (%): calc. for $C_{64}H_{82}N_8O_{11}S_2$ (**1**·H_2O): C, 63.87; H, 6.87; N, 9.31; S, 5.33. Found: C, 63.65; H, 6.74; N, 9.33; S, 5.24.

Functionalization of CdSe-QDs and Ag-NPs with dithiol 1

TOPO capped **CdSe-QDs** (25 mg) or **Ag-NPs** (5 mg) were weighed in a flask, followed by the addition of 2 mL solution of 6 mg complex **1** in dichloromethane. It was stirred for 18 h. After this, the reaction mixture was evaporated to dryness. The obtained conjugate was characterized by UV-Vis spectroscopy, FTIR spectroscopy, XRD and TEM (see Results and discussion for more details).

Z-Scan measurements

The nonlinear optical activities of phthalocyanine **1** and its nanoconjugates **1-CdSe** and **1-Ag** were tested using the open aperture *Z*-scan technique using eqn (1).[5]

$$T_{Norm}(z) = \frac{1}{1 + \left(\frac{\beta_{eff} L_{eff} I_0}{1 + (z/z_0)^2}\right)} \quad (1)$$

where β_{eff} is the effective intensity dependent nonlinear two photon absorption coefficient, I_0 is the intensity of the beam at the focus. z and z_0 are the sample positions with respect to the input intensity and the Rayleigh length (defined by using $\pi w_0^2/\lambda$, where λ is the wavelength of the laser beam and w_0 is the beam waist at the focus (z = 0)), respectively. L_{eff} is the effective thickness of the sample and is given by using eqn (2).

$$L_{eff} = \frac{1 - e^{-\alpha L}}{\alpha} \quad (2)$$

where α is the linear absorption coefficient and L is the thickness of the sample. The imaginary component of the third order optical susceptibility (Im[$\chi^{(3)}$] in esu)[8,14] is directly proportional to β_{eff} *via* eqn (3):

$$\mathrm{Im}[\chi^{(3)}] = \frac{(n^2 \varepsilon_0 c \lambda \beta_{eff})}{(2\pi)} \quad (3)$$

In eqn (3), c and n, respectively, are the speeds of light in vacuum and the linear refractive index, respectively, ε_0 is the permittivity of free space and λ is the wavelength of the laser light.

At a molecular level, there is a direct correlation of $\mathrm{Im}[\chi^{(3)}]$ with the hyperpolarizability γ (which provides the nonlinear absorption per mole of the sample) *via* the relationship shown in eqn (4):[8,52]

$$\gamma = \frac{\mathrm{Im}[\chi^{(3)}]}{N^{*}f^{4}} \quad (4)$$

where $N^{*} = C_{\mathrm{mol}}N_{\mathrm{A}}$ (with C_{mol} being the concentration of the active species in the triplet state in moles) and f represents the Lorenz local field factor and is given by eqn (5):

$$f = \frac{n^{2}+2}{3} \quad (5)$$

By definition, the limiting threshold (I_{lim}/J cm^{-2}) is the input fluence at which the output fluence is 50% of the linear transmission.[53,54] The results were found to fit into two photon absorption equation.

Conflicts of interest

There are no conflicts to declare.

Acknowledgements

This work was supported by the Department of Science and Technology (DST), the National Research Foundation (NRF), the South Africa through DST/NRF South African Research Chairs Initiative for Professor of Medicinal Chemistry and Nanotechnology (UID = 62620) as well as Rhodes University. This work was also supported by the Programs of Russian Academy of Sciences.

Notes and references

1 D. Dini, M. J. F. Calvete and M. Hanack, *Chem. Rev.*, 2016, **116**, 13043–13233.
2 J. E. Riggs and Y.-P. Sun, *J. Phys. Chem. A*, 1999, **103**, 485–495.
3 Y.-P. Sun and J. E. Riggs, *Int. Rev. Phys. Chem.*, 1999, **18**, 43–90.
4 L. De Boni, D. S. Corrêa and C. R. Mendonça, in *Advances in Lasers and Electro Optics*, ed. N. Costa and A. Cartaxo, InTech, 2010, pp. 33–58.
5 R. L. Sutherland, *Handbook of Nonlinear Optics*, *Revised and Expanded*, Marcel Dekker, Inc., New York, Basel, 2nd edn, 2003.
6 J. L. Bredas, C. Adant, P. Tackx, A. Persoons and B. M. Pierce, *Chem. Rev.*, 1994, **94**, 243–278.
7 D. Dini, M. Barthel and M. Hanack, *Eur. J. Org. Chem.*, 2001, **2001**, 3759–3769.
8 Y. Chen, M. Hanack, Y. Araki and O. Ito, *Chem. Soc. Rev.*, 2005, **34**, 517–529.
9 J. W. Perry, D. Alvarez, I. Choong, K. Mansour, S. R. Marder and K. J. Perry, *Opt. Lett.*, 1994, **19**, 625.
10 A. G. Martynov, Y. G. Gorbunova and A. Y. Tsivadze, *Russ. J. Inorg. Chem.*, 2014, **59**, 1635–1664.
11 V. N. Nemykin, S. V. Dudkin, F. Dumoulin, C. Hirel, A. G. Gürek and V. Ahsen, *ARKIVOC*, 2014, **2014**, 142.
12 G. de la Torre, P. Vázquez, F. Agulló-López and T. Torres, *J. Mater. Chem.*, 1998, **8**, 1671–1683.
13 G. de la Torre, P. Vázquez, F. Agulló-López and T. Torres, *Chem. Rev.*, 2004, **104**, 3723–3750.
14 E. M. García-Frutos, S. M. O'Flaherty, E. M. Maya, G. de la Torre, W. Blau, P. Vázquez and T. Torres, *J. Mater. Chem.*, 2003, **13**, 749–753.
15 S. J. Mathews, S. Chaitanya Kumar, L. Giribabu and S. Venugopal Rao, *Opt. Commun.*, 2007, **280**, 206–212.
16 V. Chauke, M. Durmuş and T. Nyokong, *J. Photochem. Photobiol., A*, 2007, **192**, 179–187.
17 J. S. Shirk, R. G. S. Pong, S. R. Flom, H. Heckmann and M. Hanack, *J. Phys. Chem. A*, 2000, **104**, 1438–1449.
18 J. Britton, A. G. Martynov, D. O. Oluwole, Y. G. Gorbunova, A. Y. Tsivadze and T. Nyokong, *J. Porphyrins Phthalocyanines*, 2016, **20**, 1296–1305.
19 W. Jia, E. P. Douglas, F. Guo and W. Sun, *Appl. Phys. Lett.*, 2004, **85**, 6326–6328.
20 S. Qu, C. Du, Y. Song, Y. Wang, Y. Gao, S. Liu, Y. Li and D. Zhu, *Chem. Phys. Lett.*, 2002, **356**, 403–408.
21 N. Venkatram, D. N. Rao and M. a. Akundi, *Opt. Express*, 2005, **13**, 867–872.
22 R. B. Martin, M. J. Meziani, P. Pathak, J. E. Riggs, D. E. Cook, S. Perera and Y. P. Sun, *Opt. Mater.*, 2007, **29**, 788–793.
23 I. L. Medintz, H. T. Uyeda, E. R. Goldman and H. Mattoussi, *Nat. Mater.*, 2005, **4**, 435–446.
24 M. C. Daniel and D. Astruc, *Chem. Rev.*, 2004, **104**, 293–346.
25 J. Britton, C. Litwinski, M. Durmuş, V. Chauke and T. Nyokong, *J. Porphyrins Phthalocyanines*, 2011, **15**, 1239–1249.
26 K. Sanusi, S. Khene and T. Nyokong, *Opt. Mater.*, 2014, **37**, 572–582.
27 J. Britton, M. Durmuş, V. Chauke and T. Nyokong, *J. Mol. Struct.*, 2013, **1054–1055**, 209–214.
28 A. Ulman, *Chem. Rev.*, 1996, **96**, 1533–1554.
29 J. C. Love, L. a. Estroff, J. K. Kriebel, R. G. Nuzzo and G. M. Whitesides, *Chem. Rev.*, 2005, **105**, 1103–1170.
30 T. R. E. Simpson, D. A. Russell, I. Chambrier, M. J. Cook, A. B. Horn and S. C. Thorpe, *Sens. Actuators, B*, 1995, **29**, 353–357.
31 N. Nombona, E. Antunes, C. Litwinski and T. Nyokong, *Dalton Trans.*, 2011, **40**, 11876.
32 X. Huang, Y. Liu, S. Wang, S. Zhou and D. Zhu, *Chem. – Eur. J.*, 2002, **8**, 4179–4184.
33 D. O. Oluwole, A. V. Yagodin, N. C. Mkhize, K. E. Sekhosana, A. G. Martynov, Y. G. Gorbunova, A. Y. Tsivadze and T. Nyokong, *Chem. – Eur. J.*, 2017, **23**, 2820–2830.

34 T. Kimura, T. Suzuki, Y. Takaguchi, A. Yomogita, T. Wakahara and T. Akasaka, *Eur. J. Org. Chem.*, 2006, 1262–1270.
35 I. Chambrier, M. J. Cook and D. A. Russell, *Synthesis*, 1995, 1283–1286.
36 K. P. Birin, Y. G. Gorbunova and A. Y. Tsivadze, *Russ. J. Inorg. Chem.*, 2007, **52**, 191–196.
37 N. Sheng, Y. Zhang, H. Xu, M. Bao, X. Sun and J. Jiang, *Eur. J. Inorg. Chem.*, 2007, 3268–3275.
38 A. G. Martynov, I. V. Nefedova, Y. G. Gorbunova and A. Y. Tsivadze, *Mendeleev Commun.*, 2007, **17**, 66–67.
39 R. L. A. David and J. A. Kornfield, *Macromolecules*, 2008, **41**, 1151–1161.
40 S. Shinkai, K. Inuzuka, O. Miyazaki and O. Manabe, *J. Org. Chem.*, 1984, **49**, 3440–3442.
41 F. Goethals, D. Frank and F. Du Prez, *Prog. Polym. Sci.*, 2017, **64**, 76–113.
42 K. P. Birin, V. N. Chugunov, A. A. Krapivenko, Y. G. Gorbunova and A. Y. Tsivadze, *Macroheterocycles*, 2014, **7**, 153–161.
43 R. Jenkins and R. Snyder, *Introduction to X-Ray Powder Diffractometry*, Wiley, 1996.
44 M. Ohmori, C. Nakano, A. Fujii, Y. Shimizu and M. Ozaki, *J. Cryst. Growth*, 2016, 0–1.
45 Y. G. Gorbunova, A. D. Grishina, A. G. Martynov, T. V. Krivenko, A. A. Isakova, V. V. Savel'ev, S. E. Nefedov, E. V. Abkhalimov, A. V. Vannikov and A. Y. Tsivadze, *J. Mater. Chem. C*, 2015, **3**, 6692–6700.
46 A. G. Martynov, I. V. Biryukova, Y. G. Gorbunova and A. Y. Tsivadze, *Russ. J. Inorg. Chem.*, 2004, **49**, 358–363.
47 A. G. Martynov, Y. G. Gorbunova, S. E. Nefedov, A. Y. Tsivadze and J.-P. Sauvage, *Eur. J. Org. Chem.*, 2012, **2012**, 6888–6894.
48 X. D. Luo, U. Farva, N. T. N. Truong, K. S. Son, P. S. Liu, C. Adachi and C. Park, *J. Cryst. Growth*, 2012, **339**, 22–30.
49 D. O. Oluwole, E. Prinsloo and T. Nyokong, *Polyhedron*, 2016, **119**, 434–444.
50 G. R. Fulmer, A. J. M. Miller, N. H. Sherden, H. E. Gottlieb, A. Nudelman, B. M. Stoltz, J. E. Bercaw and K. I. Goldberg, *Organometallics*, 2010, **29**, 2176–2179.
51 K. Sanusi, E. Antunes and T. Nyokong, *Dalton Trans.*, 2014, **43**, 999–1010.
52 D. Dini and M. Hanack, in *The Porphyrin Handbook*, ed. K. M. Kadish, K. M. Smith and R. Guiard, Elsevier, 2003, pp. 1–36.
53 F. Li, Z. He, M. Li and P. Lu, *Mater. Lett.*, 2013, **111**, 81–84.
54 Y. Chen, L. Gao, M. Feng, L. Gu, N. He, J. Wang, Y. Araki, W. Blau and O. Ito, *Mini-Rev. Org. Chem.*, 2009, **6**, 55–65.